Reactions of nitric oxide with mitochondrial cytochrome *c*: a novel mechanism for the formation of nitroxyl anion and peroxynitrite

Martyn A. SHARPE and Chris E. COOPER[1]

Department of Biological Sciences, Central Campus, University of Essex, Wivenhoe Park, Colchester CO4 3SQ, U.K.

The aerobic reactions of nitric oxide with cytochrome *c* were analysed. Nitric oxide (NO) reacts with ferrocytochrome *c* at a rate of 200 M^{-1} s^{-1} to form ferricytochrome *c* and nitroxyl anion (NO^-). Ferricytochrome *c* was detected by optical spectroscopy; NO^- was detected by trapping with metmyoglobin (Mb^{3+}) to form the EPR-detectable Mb–nitrosyl complex, and by the formation of dimers in yeast ferrocytochrome *c* via cross-linking of the free cysteine residue. The NO^- formed subsequently reacted with oxygen to form peroxynitrite, as measured by the oxidation of dihydrorhodamine 123. NO binds to ferricytochrome *c* to form the ferricytochrome *c*−NO complex. The on-rate for this reaction is $1.3 \pm 0.4 \times 10^3$ $M^{-1} \cdot s^{-1}$, and the off-rate is 0.087 ± 0.054 s^{-1}. The dissociation constant (K_d) of the complex is 22 ± 7 μM. These reactions of NO with cytochrome *c* are likely to be relevant to mitochondrial metabolism of NO. Ferricytochrome *c* can act as a reversible sink for excess NO in the mitochondria. The reduction of NO to NO^- by ferrocytochrome *c* may play a role in the irreversible inhibition of mitochondrial oxygen consumption by peroxynitrite. It is generally assumed that peroxynitrite would be formed in mitochondria via the reaction of NO with superoxide. The finding that NO^- is formed from the reaction of NO and ferrocytochrome *c* provides a means of producing peroxynitrite in the absence of superoxide, via the reaction of NO^- with oxygen.

INTRODUCTION

Nitric oxide (NO) is a biologically important signalling molecule [1,2]. The half-life ($t_{\frac{1}{2}}$) of NO *in vivo* varies, from a few minutes to a few hundred milliseconds, in tissues and is pO_2-dependent [3,4]. An increase in the intracellular NO concentration is implicated in tissue damage following an hypoxic/ischaemic event [5,6]. Irreversible tissue damage in various disease states, including stroke, heart disease and lung injury [7–10], has been suggested to require not only NO, but also the production of peroxynitrite ($ONOO^-$) from the reaction of superoxide ($O_2^{\cdot -}$) and NO. $ONOO^-$ is a strong oxidant capable of producing hydroxide and other cytotoxic radicals [11]. These radicals are capable of a number of adverse chemical reactions, including lipid peroxidation, thiol oxidation, tyrosine nitration, DNA hydroxylation and the oxidation of iron–sulphur centres. It has been suggested that $ONOO^-$ can also be formed by the reaction of nitroxyl anion (NO^-) with O_2 [12], although this reaction proceeds at a slower rate than that of NO and $O_2^{\cdot -}$ (5.7×10^7 $M^{-1} \cdot s^{-1}$ and 6.7×10^9 $M^{-1} \cdot s^{-1}$ respectively [13]). However, O_2 concentrations *in vivo* are many orders of magnitude higher than those of O_2^- (between 5–200 μM and < 66 pM respectively [14]). Therefore the formation of NO^- *in vivo* could have important consequences for the production of $ONOO^-$.

NO is a potent reversible inhibitor of mitochondrial cytochrome *c* oxidase, in the steady state [15–19]. It has been hypothesized that the intracellular NO concentration may control mitochondrial electron flux *in vivo* [20]. Mitochondria have been implicated as a potential source of NO metabolism [21]. Isolated cytochrome *c* oxidase metabolizes NO to N_2O at low oxygen tensions, and to NO_2 at higher oxygen tensions [22,23]. However, this is unlikely to be a major pathway of NO metabolism *in vivo*, as the major product is NO_2^- [4,24].

We therefore examined the decay of NO in the presence of purified cytochrome *c* and cytochrome *c* oxidase, under steady-state conditions. We report that NO is rapidly metabolized by the substrate of cytochrome *c* oxidase, cytochrome *c*. Cytochrome *c* catalyses the reduction of NO to NO^-. The production of NO^- by cytochrome *c* may, in part, explain the potency of NO inhibition of cytochrome *c* oxidase *in vivo*. Additionally, the reaction of NO^- and O_2 to produce $ONOO^-$ may be important in some disease states.

EXPERIMENTAL

NO solutions were prepared by the addition of 2 M H_2SO_4 to solid $NaNO_2$ in a Kipps apparatus. The NO gas was passed through four NaOH (20%) traps (to remove NO_2), and then through a solid CO_2 trap. The gas was collected in a buffer solution that had undergone four vacuum/N_2 deoxygenation cycles. The concentration of the NO solution varied from 1.2–2 mM. The NO_2^- concentration was generally approx. 300 μM. Cytochrome *c* [horse heart cytochrome *c* , purchased from Sigma (type C-7752)] was dissolved in 1.5 ml of 100 mM K^+-Hepes/20 μM diethylenetriamine penta-acetic acid (DEPA), pH 7.0. Then either 50 mM dithionite (for ferrocytochrome c) or 10 mM ferricyanide (for ferricytochrome *c*) was added, and the solutions were incubated for 30 min. The solutions were then passed down a Sephadex G-25 column equilibrated with 100 mM K^+-Hepes/20 μM DEPA, pH 7.0. Bovine cytochrome *c* oxidase was purified according to the method of Kuboyama et al. [25], with Tween 80 substituting for Emasol [25].

The NO concentration was measured using a World Precision Instruments (WPI) ISO-200 NO electrode connected to a WPI ISO−NO Mark II NO meter. The data was collected via a MacLab (ADInstruments) data collection interface, into a PowerMac 8200 computer. The NO decay curves were analysed using the Maclab data collection and analysis package chart, version 3.5.2. The electrode was place in a 5 ml thermostatically jacketed reaction chamber, which also housed a Clark-type O_2

Abbreviations used: DEPA, diethylenetriamine penta-acetic acid; TMPD, *N,N,N′,N′*-tetramethyl-*p*-phenylenediamine; $Mb^{(3+)}$, (met)myoglobin.

[1] To whom correspondence should be addressed (e-mail ccooper@essex.ac.uk).

electrode (Rank Bros.). The NO electrode was calibrated by filling the reaction chamber with KI/H_2SO_4 (0.1 M), and titrating with stock solutions of NO_2^-. The response time of the NO electrode was determined following the addition of NO to an anaerobic chamber; the $t_{\frac{1}{2}}$ for the rise in NO concentration was less than 5 s. The initial rise in NO concentration over the first 40 s (see Figures 1, 2 and 9) therefore represents this electrode-response time, but the rate of NO decay is too slow to be affected by the electrode response. At the relatively high constant oxygen concentrations and low NO concentrations used in Figures 1, 2 and 9, we found the decay of NO to be a mono-exponential process [3], allowing simple half-lives and exponential-decay rates to be calculated.

Nitrite was assayed using the Griess reaction. 100 μl samples or standards were added to 500 μl of 1 % (w/v) sulphanilamide in 5 % (v/v) phosphoric acid and 500 μl 0.15 napthylenediamine hydrochloride. The absorbance was recorded at 540 nm, and the assay was calibrated using nitrite standards. Optical spectra were recorded using a Hewlett–Packard HP8453 diode-array spectrophotometer. EPR spectroscopy was performed using a Varian E-line Century Series EPR spectrometer. The samples were measured at 77 K using a quartz-finger Dewar. In the wide-sweep spectra (see Figure 5) the centre field was 2331 G, sweep width 4000 G, microwave frequency 9.26 GHz and microwave power 45 mW. The myoglobin (Mb)–nitrosyl ($Mb^{2+}-NO$) narrow-sweep spectrum (see Figure 6) was recorded with a centre field of 3214 G, sweep width 400 G, microwave frequency 9.26 GHz and microwave power 45 mW.

Direct reduction of metmyoglobin (Mb^{3+}) by ferrocytochrome *c* would compromise the use of the Mb^{3+} conversion into nitrosyl Mb as a unique measure of NO^- formation. The rate constant for this reduction was therefore calculated as follows: 60 μM Mb^{3+} (in 100 mM K^+-Hepes, pH 7.0) was degasssed three times and flushed with nitrogen gas. This solution was carefully titrated, initially with 10 μM aliquots of dithionite, to produce deoxyMb with no excess of dithionite. 50 μM ferricytochrome *c* was then added. The spectral changes were recorded continuously in the diode-array spectrophotometer for 2 min, after which 150 μM ferricyanide and 1mM dithionite were added successively to generate the spectra of the fully oxidized and fully reduced species respectively. Changes in the Mb redox state were monitored at 503–527 nm and changes in the cytochrome *c* redox state at 519–615 nm. The data were fitted as a second-order process, yielding a bimolecular rate constant of 458 $M^{-1}\cdot s^{-1}$ for the forward reaction. The equilibrium constant for the deoxyMb-catalysed oxidation of ferricytochrome *c* was calculated from the respective redox potentials (cytochrome *c*, +270 mV; Mb, +50 mV) to be 4640. Therefore the reverse reaction, i.e. Mb^{3+} reduction by ferrocytochrome *c*, has a rate constant of approx. 0.1 $M^{-1}\cdot s^{-1}$. Under the conditions of the EPR-trapping experiment (see Figure 6), this means that the reduction of 10 % of the Mb^{3+} present would have taken approx. 4 h, whereas the sample was frozen within 10 min.

It was found that approx. 10 % of *Saccharomyces cerevisiae* cytochrome *c* from Sigma (type C-2436) was present as a dimeric form in the bottle. In order to determine whether NO could dimerize yeast ferrocytochrome *c*, it was first necessary to remove any preformed dimers in the purified protein. Therefore 10 mM yeast cytochrome *c* was incubated with 100 mM ascorbate and 200 mM dithiothreitol (in 100 mM Hepes/20μM DEPA, pH 7.0) at room temperature for 30 min to reduce and monomerize the cytochrome *c*. The monomeric ferrocytochrome *c* was then separated from the reductants using a Sepharose-2B column. 100 μl of 1.5 mM yeast or horse heart ferrocytochrome *c* was then placed in Eppendorf tubes sealed with Suba Seals, and 100 μl of 2 mM NO or buffer added. 10 μl of the assay mixture was then assayed by SDS/PAGE (10 % gels). The gels were stained with Coomassie Blue.

Dihydrorhodamine 123 (Molecular Probes) oxidation was measured by the fluorescence increase upon rhodamine 123 formation using a Perkin–Elmer LS50B spectrofluorimeter, with $\lambda_{excitation}$ 503 nm, and $\lambda_{emission}$ 526 nm. The latter is isosbestic for the oxidation of ferrocytochrome *c*; separate studies on the effect of ferricytochrome *c* oxidation upon the fluorescence of rhodamine 123 under these conditions revealed that the changes were much smaller than those observed following the addition of NO to ferrocytochrome *c* (see Figure 8).

The kinetic and dissociation constants for NO binding to ferricytochrome *c* were calculated as follows: the amount of free NO was measured using the NO electrode following addition of 5μM NO to differing concentrations of excess ferricytochrome *c*. As the rate of NO binding to ferricytochrome *c* was significantly faster than the non-enzymic NO metabolism by oxygen, the effects of the latter were ignored. As a single molecule of NO is known to bind to ferricytochrome *c*, the amount of bound NO was assumed to equal the amount of bound ferricytochrome *c*. A corrected free ferricytochrome *c* concentration was then plotted against the [NO] bound (in fact this correction only makes a small difference, as the cytochrome *c* is in excess and therefore the bound concentration is a small fraction of the free concentration). The data provided a good fit to a simple rectangular hyperbola; the K_d was calculated ($\pm$the 95 % confidence intervals) following non-linear regression analysis using a Marquardt algorithm. This value was checked by measuring the binding spectrophotometrically. In this case, the $c^{3+}-NO$-induced spectral change at 560–540 nm was used to determine the amount of NO bound following the addition of different concentrations of excess NO to 10 μM ferricytochrome *c*. A similar correction as before was used to calculate the amount of free NO present and this was plotted against $\Delta A_{560-540}$ (proportional to the bound complex). The K_d calculated from the resulting plot was identical with that measured when the cytochrome *c* was in excess. The on- and off-rates for cytochrome *c* binding to NO were calculated following the addition of varying concentrations of NO to 10 μM ferricytochrome *c*. At least a tenfold excess of NO over ferricytochrome *c* was used to ensure pseudo-first-order conditions. The rate of complex formation (using the 560–540 nm wave pair) fitted a single exponential time course. This rate was then plotted against the NO concentration. The slope of this graph yielded the on-rate, and the intercept on the *y*-axis gave the off-rate. Dividing the off-rate by the on-rate yielded a K_d not significantly different from that determined by the equilibrium measurements.

The deconvolution of the chromophore concentration changes that occurred when NO was added to ferrocytochrome *c* was performed by linear additions of varying amounts of the purified spectra of ferrocytochrome *c*, ferricytochrome *c* and the c^{3+}–NO complex. The sum of the least-squares difference between the model and the experimental data was minimized using the quasi-Newton iterative procedure in the Solver function in Microsoft Excel 5.0. Initial guesses were obtained manually, and the iterative fit was then performed using forward differencing for the estimations of the partial derivatives. The residuals of this fit did not correspond to any obvious spectral feature. Singular Value Decomposition (PC-Pro K, Applied Photophysics) analysis confirmed that there were only three major spectral components that varied in the data set, but global analysis could not converge on a fit using the simple model described in the text. A kinetic simulation of the interaction of ferrocytochrome *c* with NO was performed using PC-Pro K to perform numerical integrations of

the differential equations described in the text, using the rate constants in the legend to Figure 12.

Unless otherwise indicated, all experiments were performed at 30 °C in aerobic (air-saturated) solutions of 100 mM K^+-Hepes, pH 7.0, in the presence of the metal chelator DEPA (20 μM).

RESULTS

The effect of actively respiring cytochrome *c* oxidase on the decay of NO was studied in air-saturated buffer solution. Cytochrome oxidase is normally assayed in the presence of the electron donors ascorbate, *N*,*N*,*N*′,*N*′-tetramethyl-*p*-phenylenediamine (TMPD) and cytochrome *c*. Figure 1 shows the effect of these donors, in the presence and absence of cytochrome oxidase, on the decay of 5 μM NO. In the control, NO decays slowly ($t_{\frac{1}{2}}$ approx. 200 s); this is much slower than the *in vivo* rate, and is similar to the rate seen in aerobic buffer solutions [3,4]. The decay is much more rapid in the presence of ascorbate, TMPD and cytochrome *c* ($t_{\frac{1}{2}}$ approx. 35 s). The presence of cytochrome *c* oxidase does not increase the rate of NO decay; indeed, the addition of cytochrome oxidase makes the mixture of ascorbate, TMPD and cytochrome *c* less reactive to the NO ($t_{\frac{1}{2}}$ approx. 50 s). Under these conditions, O_2 consumption by cytochrome oxidase was completely inhibited. These results suggest that aerobic NO metabolism by purified cytochrome oxidase is predominantly due to the electron donors to the enzyme, rather than the enzyme itself.

Of the three electron donors described in Figure 1, only ferrocytochrome *c* is physiologically present in mitochondria.

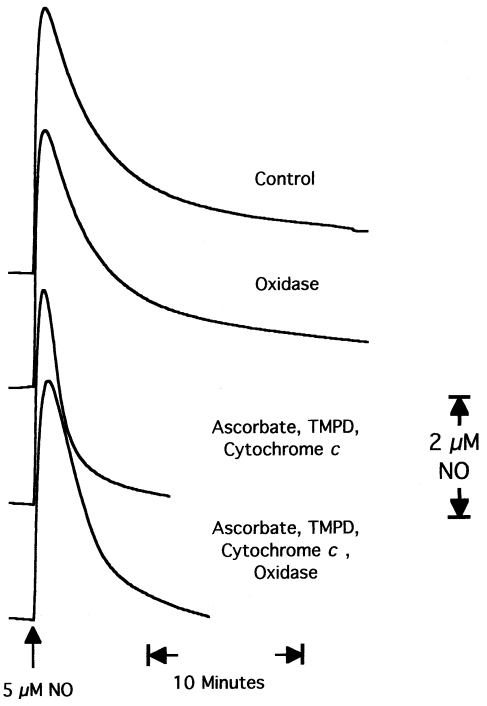

Figure 1 Decay of NO in aerobic buffer in the presence of cytochrome *c* and cytochrome *c* oxidase

5 ml of 100 mM K^+-Hepes, pH 7.0 at 30 °C was placed in a thermally jacketed, stirred incubation chamber. 5 μM NO was added in the presence of the indicated reagents: buffer control; +oxidized cytochrome oxidase (200 nM); +ascorbate (20 mM), TMPD (300 μM) and cytochrome *c* (45 μM); +ascorbate (20 mM), TMPD (300 μM), cytochrome *c* (45 μM) and cytochrome oxidase (200 nM).

We therefore examined the effect of increasing concentrations of ferrocytochrome *c* on the decay of 5 μM NO (Figure 2a, and plotted logarithmically in Figure 2b). Although the autoxidation of NO by O_2 is a third-order process, under these conditions (low NO concentrations and fixed high O_2 concentrations) the rate approximates to a first-order process [3]. After the initial equilibration period, caused by the response time of the NO electrode, the slow decay of NO can be fitted to a first-order process. In the presence of increasing concentrations of ferrocytochrome *c*, the rate of NO decay increases (Figure 2c). Assuming that pseudo-first-order conditions apply at the higher ferrocytochrome *c* concentrations, the slope of this graph yields a rate constant for the reaction of NO with ferrocytochrome *c* of approx. 200 $M^{-1}\cdot s^{-1}$. Extrapolating the linear portion of the logarithmic plot to zero time reveals that a fraction of the NO is removed very rapidly by ferrocytochrome *c* under these conditions. This fraction is proportional to the ferrocytochrome *c* concentration, and represents about 3% of the amount added (Figure 2d). Monomeric ferrocytochrome *c* binds NO reversibly [26,27], but this process occurs very slowly (over many hours) at this pH [28]. However, a small fraction of cytochrome *c* polymers are present in this kind of preparation; as these can bind CO rapidly [29] it is likely that they can also bind NO, and are therefore responsible for the observed small fraction of NO binding.

In order to determine the reaction products, we measured the effect of NO on the optical spectrum of ferrocytochrome *c* (Figure 3). The predominant transition observed is the formation of oxidized cytochrome *c* with isosbestic points at 541 and 556 nm. Increasing the NO concentration increases the amount of cytochrome *c* oxidation (Figure 4), although the ferrocytochrome *c* is never fully oxidized. Following the initial oxidation, there is a slow re-reduction of the cytochrome *c*. Re-reduction occurs at a faster rate at higher NO concentrations (results not shown). As expected at this pH [27], there is no evidence in the optical spectra for the formation of the ferrous–NO complex. However, we do detect a small fraction of a species absorbing at 562 nm (inset to Figure 3), consistently with some formation of the ferric−NO complex of cytochrome *c* [27].

What is the mechanism for the oxidation of ferrocytochrome *c* by NO? The most likely reaction of ferrocytochrome with NO is the reduction of NO to NO^-. This reaction has been shown to be catalysed by superoxide dismutase [30] (midpoint potential 420 mV), and by ferrous ion in acidic solution [31]. The reverse reaction (nitroxyl anion reduction of ferrocytochrome *c*) has also been demonstrated [32]. The midpoint potential of the c^{2+}/c^{3+} couple is approx. 270 mV; the potential of the NO/NO^- couple is not well-characterized, but indirect measurements suggest a value of 250 mV under these conditions [30,33]; thus the production of NO^- from NO and ferrocytochrome *c* is thermodynamically feasible.

We tested this hypothesis directly by using Mb^{3+} as a NO^- trap [30]. NO reacts with Mb^{3+} to produce the EPR-silent $Mb^{3+}-NO$ complex. However, NO^- reacts with Mb^{3+} to produce $Mb^{2+}-NO$ (the Mb-nitrosyl species), which gives an EPR signal centred around $g = 2$. We therefore examined the EPR spectrum of Mb^{3+} in the presence of ferrocytochrome *c* and NO (Figure 5). Ferrocytochrome *c* does not cause significant reduction of Mb^{3+}, as there is no loss of the high-spin $g = 6$ signal of Mb^{3+} in the presence of ferrocytochrome *c*. The addition of NO to Mb^{3+} causes a slight drop in the $g = 6$ signal [indicating formation of the EPR-silent $Mb^{3+}-NO$ complex (approx. 10%)]. In the presence of NO, ferrocytochrome *c* and Mb^{3+}, we see a drop in the $g = 6$ signal, and the appearance of a signal near

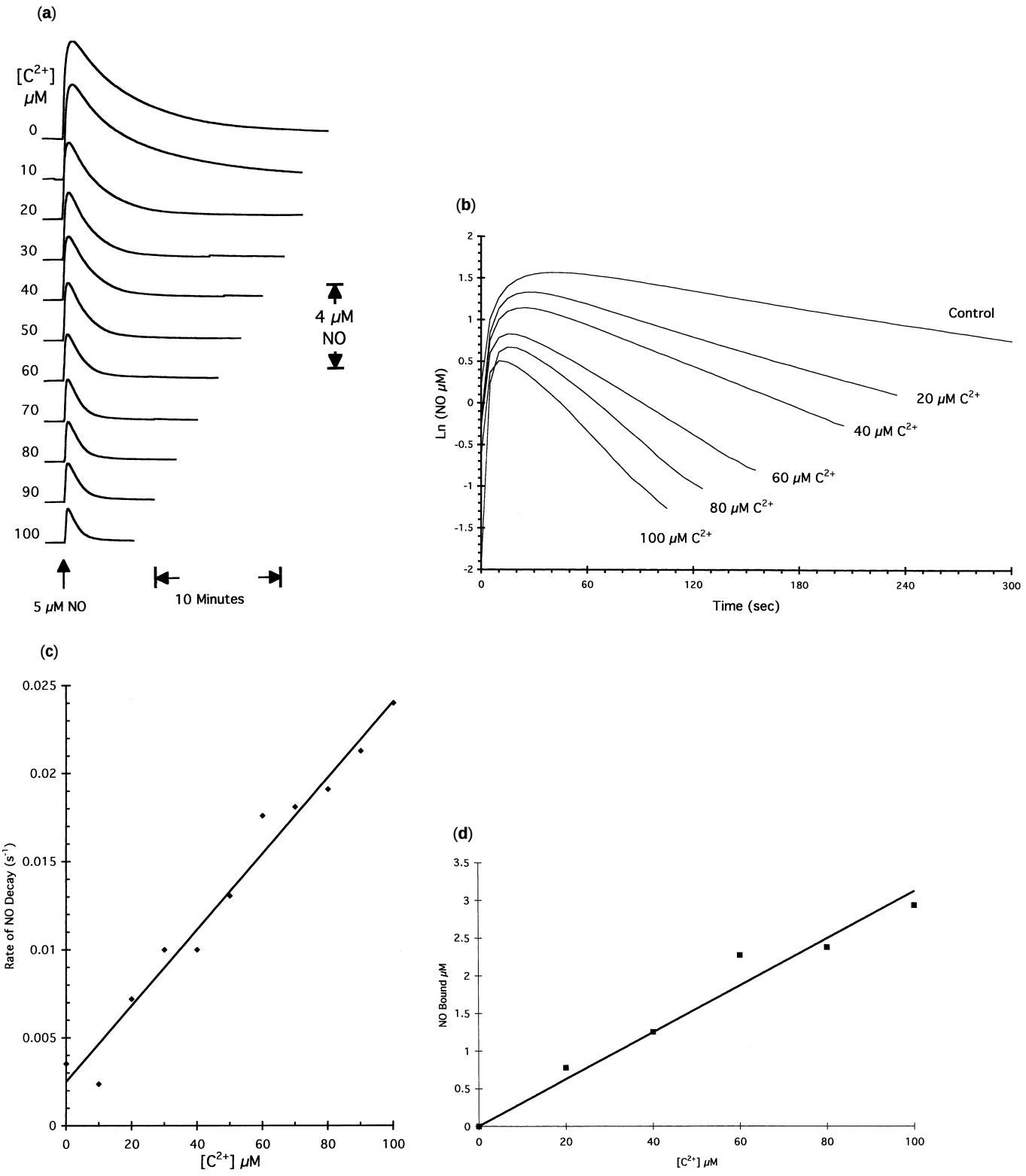

Figure 2 Rate of NO reaction with ferrocytochrome *c*

The effect of increasing concentrations of ferrocytochrome *c* on the decay of 5 μM NO is shown (**a**). Other conditions are as found in Figure 1. (**b**) illustrates the *y*-axis on a logarithmic scale. The rate of NO decay as a function of the initial ferrocytochrome *c* concentration is plotted in (**c**). The intercept of the linear portion of the logarithmic plot with the time-zero point was used to calculate the amount of NO rapidly removed from solution, and this is plotted as a function of the ferrocytochrome *c* concentration in (**d**).

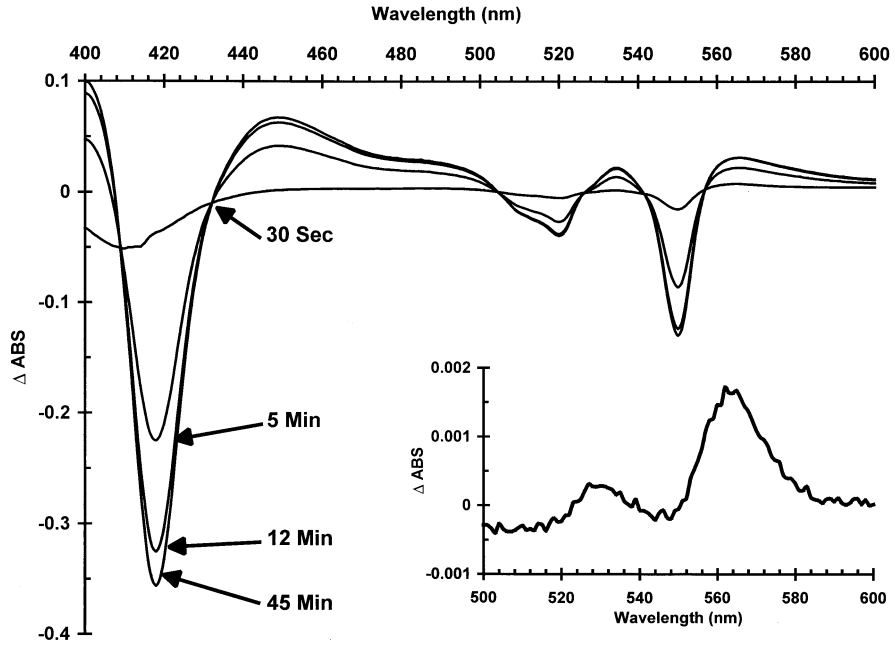

Figure 3 Effect of NO on the optical spectrum of ferrocytochrome *c*

The change in absorption spectra of 10 μM ferrocytochrome *c* following the addition of 100 μM NO. The spectrophotometer was blanked on 10 μM ferrocytochrome *c* dissolved in 100 mM K^+-Hepes, pH 7.0 at 30 °C. The inset shows optical changes consistent with the presence of the $c^{3+}-NO$ complex 12 min after NO addition. The spectrum was obtained by subtracting appprox. 95% of the spectrum taken at 45 min (when there is NO present) from the spectrum taken at 12 min.

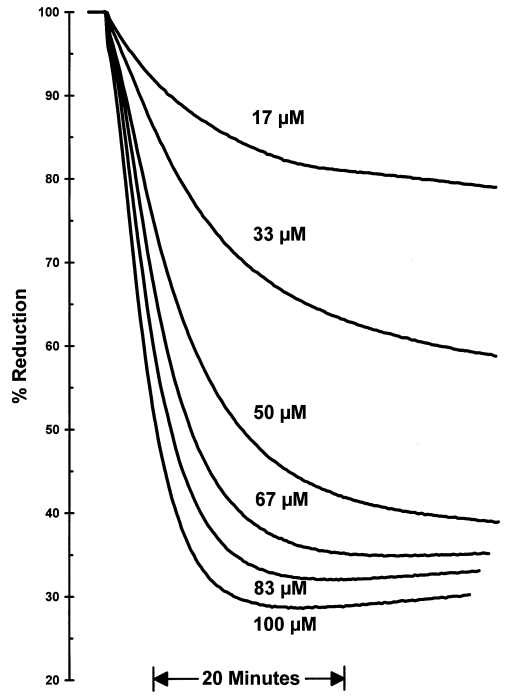

Figure 4 Rate of oxidation of ferrocytochrome *c* by NO

The effect of increasing concentrations of NO on the oxidation of 10 μM ferrocytochrome *c*. The redox state of cytochrome *c* was calculated using the 550–540 nm wave-pair. To enable the % reduction to be calculated during the time course, 100% ferricytochrome *c* was generated by the addition of ferricyanide (10 μM) at the end of each experiment.

$g = 2$. Both the position and line shape of the latter signal are the same as that of the $Mb^{2+}-NO$ species generated by mixing Mb^{3+}, dithionite and NO (Figure 6). Comparison of the two spectra reveal that 9 μM $Mb^{2+}-NO$ is formed from NO^- trapping. This represents 10% of the total Mb^{3+} added to the ferrocytochrome *c*–NO mixture. Although the ferrocytochrome–nitrosyl complex is also EPR-detectable in the $g = 2$ region [34], it has a line shape distinct from that observed in Figure 6. However, we cannot rule out the possibility that a small fraction of this complex underlies the majority $Mb^{2+}-NO$ signal detected.

A possible criticism of our method of trapping NO^- is that it may be possible that ferrocytochrome *c* reduces Mb^{3+} directly. Even if it is thermodynamically unfavourable, the presence of NO could make this reaction significant by kinetically trapping the small fraction of Mb^{2+} formed as the $Mb^{2+}-NO$ species. Clearly this would invalidate the use of Mb^{3+} as a nitroxyl-anion trap under these circumstances. We independently measured the rate of reduction of Mb^{3+} by ferrocytochrome *c* (see the Experimental section). The value calculated ($0.1\ M^{-1}\cdot s^{-1}$) is too slow for any appreciable formation of $Mb^{2+}-NO$ by this mechanism in the time frame of this experiment. Furthermore, even if this reaction were significantly faster, ferrocytochrome *c* oxidation of Mb^{3+} would be an unlikely method of $Mb^{2+}-NO$ production in the aerobic solutions used, because oxygen binding to Mb^{2+} would tend to out-compete NO binding. Thus the fact that we see $Mb^{2+}-NO$ at all in this study has mechanistic implications for the interaction of NO^- with Mb^{3+}. It suggests that the initial step must be a binding reaction, rather than electron transfer, as the formation of NO and Mb^{2+} in an aerobic solution would not be expected to lead to the nitrosyl complex (instead, oxyMb would be formed, and this would react with the NO to form Mb^{3+} with consequent nitrite production).

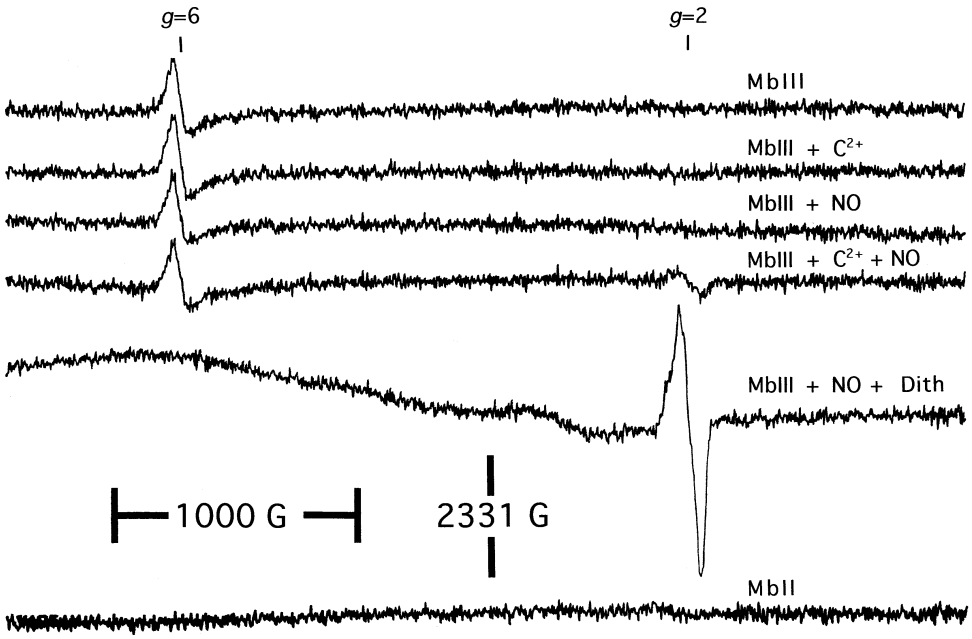

Figure 5 EPR detection of the products of the reaction of NO with ferrocytochrome *c*

The samples contained 100 mM K^+-Hepes (pH 7.0), Mb^{3+} (90 μM) and, where indicated, ferrocytochrome *c* (C^{2+}; 100 μM), and/or NO (150 μM), or NO and dithionite (1 mM). The deoxyMb spectrum, Mb^{2+}, was generated by the addition of 1 mM dithionite (Dith) to 90 μM Mb^{3+}. Samples were prepared aerobically and frozen in liquid nitrogen after 10 min.

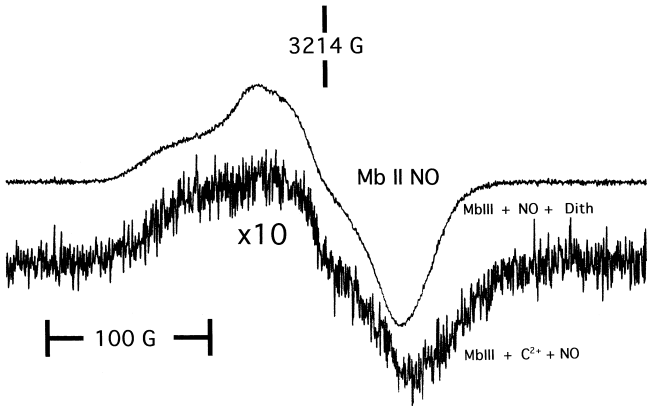

Figure 6 EPR spectra indicating NO^- trapping by Mb^{3+}

EPR spectra of nitrosyl-Mb generated from NO^- and Mb^{3+}. The upper spectrum shows 90 μM pure nitrosyl-Mb complex (generated by the addition of NO and dithionite to Mb^{3+}). The lower spectrum shows the spectrum of Mb^{3+} incubated with NO and ferrocytochrome *c* (C^{2+}). All reaction conditions were as in Figure 5. The lower spectrum was recorded at a 10 × expanded gain.

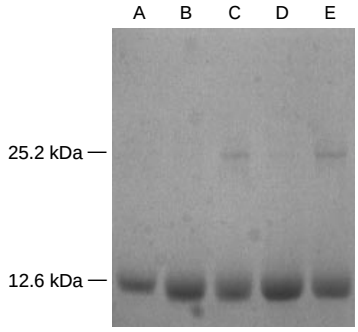

Figure 7 Cross-linking of yeast ferrocytochrome *c* by NO

Tracks present on SDS/polyacrylamide gel: (**A**) 750 μM horse heart ferrocytochrome *c* (M_r 12384) + 1 mM NO; (**B**) 750 μM yeast ferrocytochrome *c* (M_r 12588) + 1 mM NO and 20 mM cysteine; (**C**) 750 μM yeast ferrocytochrome *c* + 1 mM NO; (**D**) 750 μM yeast ferrocytochrome *c* + buffer; (**E**) 750 μM yeast ferrocytochrome *c* + 1 mM NO at low oxygen tension (1–5 μM). Note that under the denaturing conditions of this gel, the small fraction of non-covalent CO-binding polymers present in horse heart cytochrome *c* run as monomers.

Unlike NO, NO^- can react with thiols to form disulphide bridges and hydroxylamine [32]. We used this reaction as additional confirmation that ferrocytochrome *c* can oxidize NO to NO^- by making use of the free cysteine group present in yeast cytochrome *c*. The addition of NO to yeast ferrocytochrome *c* resulted in the formation of covalent cross-linked dimers (Figure 7). These were observed neither in the case of horse heart cytochrome *c* (lacking the free cysteine residue), nor if excess cysteine was present in the solution.

Reducing the oxygen concentration resulted in a slight increase in the amount of dimers formed from NO and yeast ferrocytochrome *c*. This suggested that a reaction with oxygen might be competing with the cysteine residues for the NO^- produced. One possible candidate reaction is the direct production of peroxynitrite from NO^- and oxygen. We measured peroxynitrite formation in this system by following the oxidation of dihydrorhodamine 123 to the fluorescent rhodamine 123 product [35]. Figure 8 demonstrates that this reaction occurs on a similar time scale to the oxidation of ferrocytochrome *c* by NO. Furthermore,

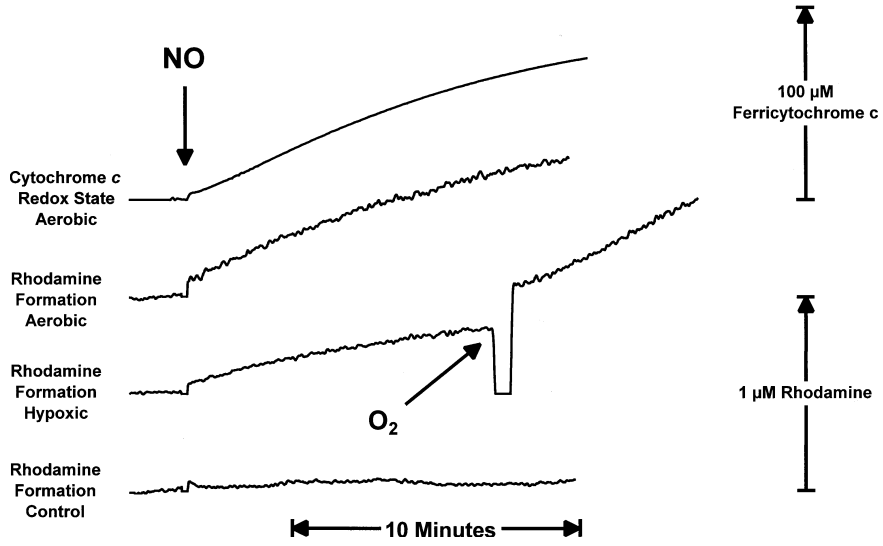

Figure 8 Dihydrorhodamine 123 oxidation by ferrocytochrome *c* and NO

Ferrocytochrome *c* was incubated in 3 ml 100 mM K^+-Hepes/20 μM DEPA in a sealed fluorescence cuvette. Dihydrorhodamine 123 was added to this mixture. At the indicated time point, 0.5 ml of a 2 mM NO solution was added. The final concentrations following the NO addition were 100 μM ferrocytochrome *c*, 3 μM dihydrorhodamine 123 and 300 μM NO. In a control sample, buffer was added instead of NO. One sample (hypoxic) was degassed three times, and nitrogen flushed to reduce the oxygen concentration to approx. 1–5 μM. Where indicated, this cuvette was flushed and mixed with a stream of O_2 gas. At the end of each experimental run, 100 μM peroxynitrite was added to completely oxidize the dihydrorhodamine 123 for calibration purposes. The rate of production of ferricytochrome *c* in the aerobic study is illustrated from a parallel optical experiment under identical conditions.

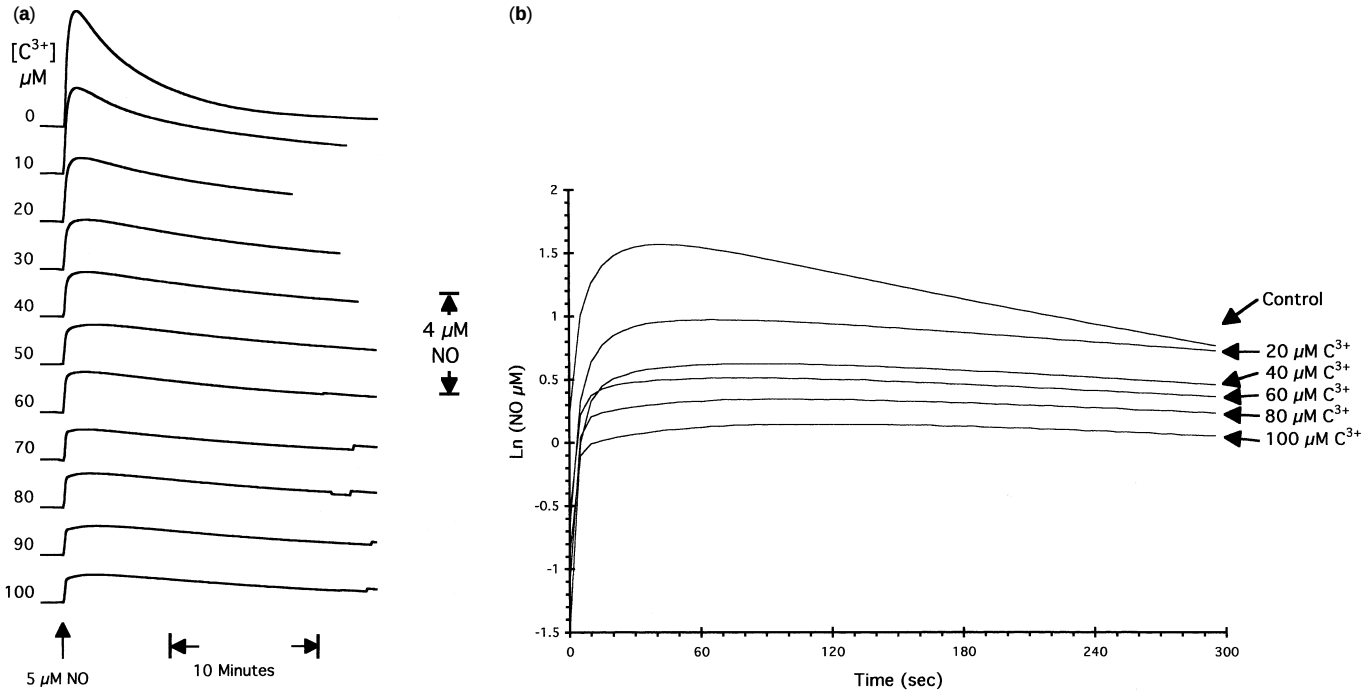

Figure 9 Removal of NO from aerobic solution by ferricytochrome *c*

(**a**) The effect of increasing concentrations of ferricytochrome *c* (C^{3+}) on the decay of 5 μM NO is shown. Other conditions are as found in Figure 1. (**b**) The *y*-axis is shown plotted as a logarithmic transformation.

the reaction rate is reduced by lowering the oxygen tension in the cuvette; this reduced rate can be accelerated by the subsequent reintroduction of oxygen.

Cytochrome *c* *in vivo* is more oxidized than reduced. Ferricytochrome *c* is also the product of the reaction of NO with ferrocytochrome *c*. Therefore we studied the effect of ferricytochrome *c* on the decay of NO concentration in aerobic solution. Figure 9(a) shows the effect of adding 5 μM NO to aerobic

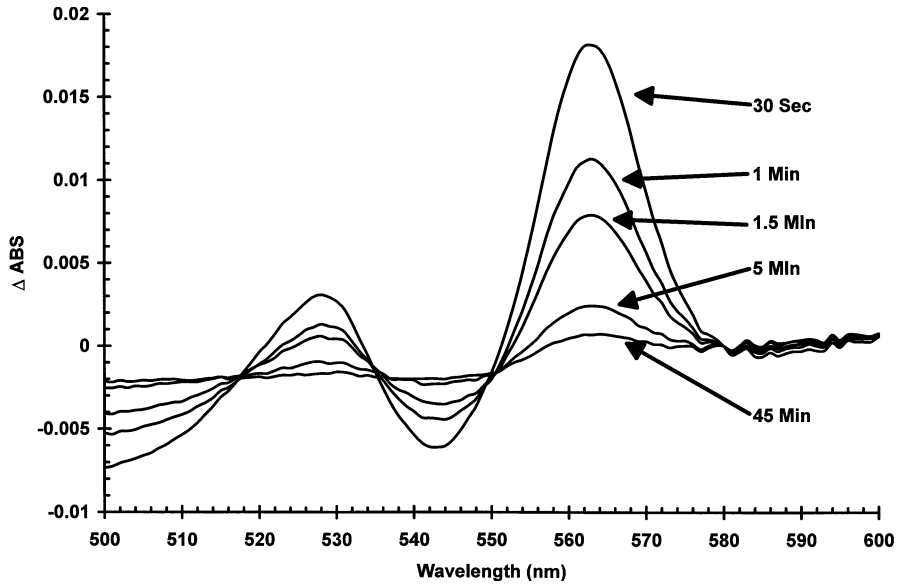

Figure 10 Optical detection of NO binding to ferricytochrome *c*

Spectra of ferricytochrome *c* following the addition of 100 μM NO. The spectra show the formation and decay of the ferricytochrome *c*—NO complex, centred at 562 nm. Conditions are as found in Figure 4, with the substitution of 10 μM ferricytochrome *c* for 10 μM ferrocytochrome *c*.

solutions of increasing concentrations of ferricytochrome *c*. The logarithmic plots (Figure 9b) show a decrease in the initial concentration of free NO as the ferricytochrome *c* concentration is increased. The presence of ferricytochrome *c* apparently decreases the subsequent rate of NO removal from the solution compared with the control. However, this effect is independent of the added ferricytochrome *c* concentration, and may be due to binding of trace elements in the buffer that enhance the rate of NO decay in the control.

The lack of any increase in the rate of NO decay in these circumstances suggests that, unlike ferrocytochrome *c*, the predominant initial reaction of ferricytochrome *c* with NO may be binding, rather than metabolism. This is indeed the case, as shown by optical spectroscopy (Figure 10). The initial spectrum of the ferricytochrome-*c*-containing solution following the addition of NO shows the appearance of a peak at 562 nm, characteristic of the $c^{3+}-NO$ complex [27]. This peak decays as NO is removed from the solution via reaction with oxygen. We examined the NO-derived products of the reaction between ferricytochrome *c* and NO, and found that the NO was essentially converted quantitatively into nitrite. Thus the most likely pathway for the decay of the optical spectrum of the ferric–NO complex is that NO is removed from the solution owing to reaction with oxygen, with a resulting shift in the equilibrium in favour of NO dissociation. The amount of the $c^{3+}-NO$ complex formed increased with increasing NO concentration and, as expected, there was a simultaneous bleaching of the 695 nm band, indicating that the methionine–Fe^{3+} band has been broken by NO binding (results not shown).

We can measure the dissociation constant of NO for ferricytochrome *c* using the data in Figure 10 (fixed NO, varying ferricytochrome *c*, electrochemical detection of free NO), or Figure 9 (fixed cytochrome *c*, varying NO, optical detection of bound NO). Figure 11 illustrates that both these methods yield an identical value for the K_d of 22 μM. The on- and off-rates for NO binding to ferricytochrome *c* can be calculated by adding excess NO to a fixed solution of ferricytochrome *c* (optical detection of $c^{3+}-NO$ complex). The on-rate is $1.3 \pm 0.4 \times 10^3\ M^{-1} \cdot s^{-1}$ and the off-rate is $0.087 \pm 0.054\ s^{-1}$.

Equations 1 and 2 therefore represent the major reactions of NO with mitochondrial cytochrome *c*:

$$NO + c^{2+} \leftrightarrow NO^- + c^{3+} \quad (1)$$

$$NO + c^{3+} \leftrightarrow c^{3+}-NO \quad (2)$$

However, a complete picture of these interactions may require some additional side reactions. In particular, the slow re-reduction of ferricytochrome *c* shown in Figure 1 is not explained by these processes. This may be linked to the fact that we also see some formation of ferrocytochrome *c* following prolonged (30 min) incubation of ferricytochrome *c* with NO. One possible reaction that might explain these phenomena is the hydration of $c^{2+}-NO^+$ (a resonance structure of the $c^{3+}-NO$ complex) to form ferrocytochrome *c*, nitrite and protons (eqns. 3 and 4):

$$c^{3+}-NO \leftrightarrow c^{2+}-NO^+ \quad (3)$$

$$c^{2+}-NO^+ + H_2O \leftrightarrow c^{2+} + NO_2^- + 2H^+ \quad (4)$$

These reactions have been suggested previously by Orii and Shimada [28] and Ehrenberg and Szczepkowski [36], although at neutral pH they are significantly slower than the processes occurring in eqns. (1) and (2). Additional complexity may ensue owing to the formation of nitroxyl anion and peroxynitrite in this system. For example, we have attempted to model the kinetics of the reactions following the addition of NO to ferrocytochrome *c* using the rate constants derived from Figures 2 and 11 and the following simple mechanism:

$$NO + c^{2+} \xrightarrow{k_{+1}} NO^- + c^{3+}$$

$$NO + c^{3+} \underset{k_{-2}}{\overset{k_{+2}}{\leftrightarrow}} c^{3+}\text{–}NO$$

$$NO \xrightarrow{k_{+3}} NO_2^-$$

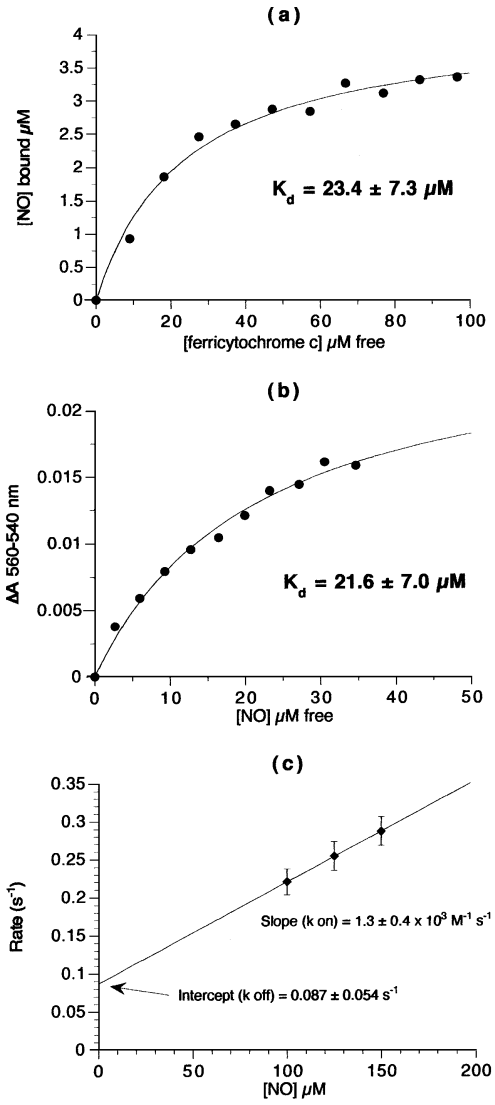

Figure 11 Measurement of kinetic and thermodynamic constants for the binding of NO to ferricytochrome *c*

(**a**) A plot of the binding of NO as a function of ferricytochrome *c* concentration is shown. The data were taken from Figure 7. (**b**) The formation of the '562' compound as a function of NO concentration is presented. 10 μM ferricytochrome *c* was incubated in 100 mM K^+-Hepes, pH 7.0 at 30 °C, and an aliquot of NO was added. (**c**) The rate of the '562' complex formation under the conditions of Figure 8 as a function of a high initial NO concentration is shown. The data are plotted as means ± S.D. ($n = 3$). The thermodynamic and kinetic analyses were as described in the Experimental section. Kinetic and dissociation constants are quoted as ± the 95% confidence value. The K_d calculated from the on- and off-rates in Figure 9(c) is 66 ± 47 μM, not significantly different from those calculated in Figures 11(a) and 11(b).

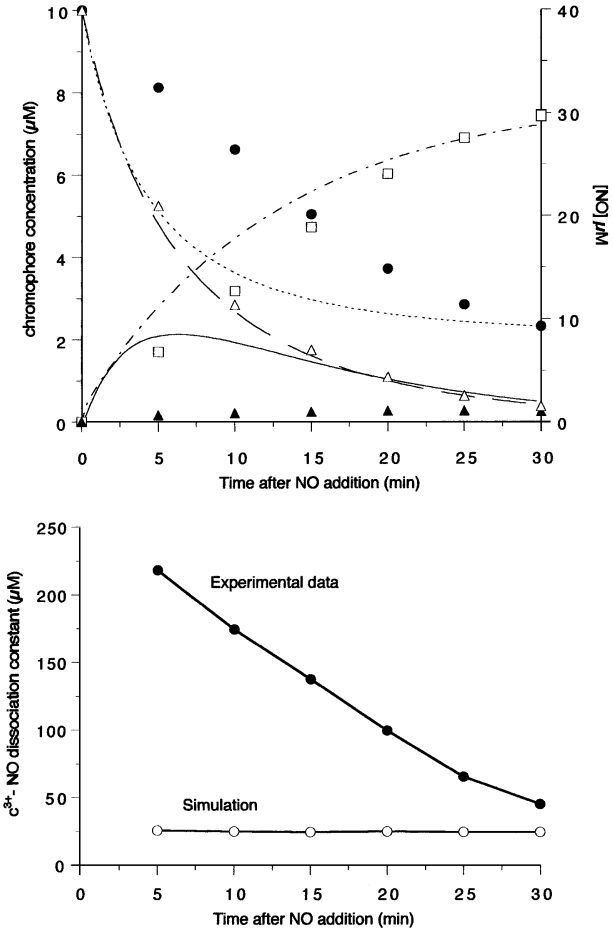

Figure 12 Simulation of NO and chromophore concentration changes following the addition of NO to ferrocytochrome *c*

(**a**) 40 μM NO was added to 10μM ferrocytochrome *c* in parallel NO electrode and optical studies. The spectra were deconvoluted to indicate the changes in oxidized and reduced cytochrome *c* and the c^{3+}—NO complex. Kinetic constants consistent with the date from Figures 2 and 11 were used to illustrate the problems with modelling all the parameters adequately in this system with the simple model described in the text. $k_{+1} = 80$ M^{-1} s^{-1}; $k_{+2} = 1300$ $M^{-1} \cdot s^{-1}$; $k_{-2} = 0.033$ s^{-1}; $k_{+3} = 0.00165$ s^{-1}. Experimental data: ferrocytochrome *c* (●), ferricytochrome *c* (□), c^{3+}—NO complex (▲) and NO (△). Simulated concentration changes: ferrocytochrome *c* (· · · · · · ·), ferricytochrome *c* (· · · · ·), c^{3+}—NO complex (-) and NO (— — — —). (**b**) Using the combined optical and NO data, plots are presented showing the apparent K_d of the ferricytochrome *c*–NO complex ($[c^{3+}]$ [NO]/$[c^{3+}$—NO]) as a function of time for the data and the simulation.

where k_{+3} represents the pseudo-first-order rate constant for the reaction of NO with oxygen under these conditions.

Figure 12(a) demonstrates that, while the levels of NO and ferricytochrome *c* can be approximately modelled, there is too much ferrocytochrome *c* and too little c^{3+}—NO complex present. This is illustrated by the fact that the c^{3+}—NO complex is out of equilibrium throughout the time course (Figure 12b); the levels of NO, ferricytochrome *c* and the complex only approach the K_d of 20 μM when the ferrocytochrome *c* and NO concentrations are significantly lowered. Clearly, additional reactions are present that depress the formation of the complex and increase the formation of ferrocytochrome *c*.

DISCUSSION

The reactions of NO with ferri- and ferro-cytochrome *c* have important implications for the inhibition of mitochondrial oxygen consumption by NO and the mitochondrial metabolism of NO. Ferrocytochrome *c* reduces NO to NO^-. NO^- is a very reactive species capable of a number of potentially cytotoxic reactions, the most important of which is the reaction with O_2 to form $ONOO^-$ [13,30]. NO^-, derived from the decomposition of Angeli's salt, is readily oxidized by ferricytochrome *c* [32]. It

therefore seems likely that the production of NO^- *in vivo* is favoured when NO concentrations are high and the cytochrome *c* pool is reduced. These conditions exist during ischaemia, when lack of oxygen results in an inability of cytochrome oxidase to oxidize cytochrome *c*, and the NO levels are increased [37,38]. The same conditions would also apply following the addition of excess NO alone to cells, even at high oxygen tensions [18,39]. This would result in inhibition of cytochrome oxidase; the susbsequent increased reduction of the cytochrome *c* pool and the presence of NO would then both favour NO^- production.

The presence and importance of NO^- *in vivo* is controversial [40,41]. This work demonstrates that it can be formed readily from the reaction of NO with a normal mitochondrial protein. What is likely to be the significance of any NO^- formed? One possibility, as demonstrated in this paper, is that the reaction of NO^- and oxygen could be an alternative mechanism for the manufacture of peroxynitrite by mitochondria in the absence of superoxide. This is important given the irreversible nature of peroxynitrite inhibition of mitochondrial oxygen consumption, compared with its reversible inhibition by NO. Our finding that NO^- reacts with Mb^{3+} via an initial binding, rather than an electron-transfer reaction, may have important implications for the formation *in vivo* of haem nitrosyl species. For example, it is possible that in highly aerobic arterial blood, some of the nitrosyl haemoglobin formed following increases in NO production [42] may arise from the reaction of NO^- with methaemoglobin, rather than solely from the reaction of NO with deoxyhaemoglobin. NO^- itself may be a potent inhibitor of some enzyme activities. In particular, the ability to form stable ferrous nitrosyl complexes from ferric haem enzymes (witness the EPR-trapping experiment) may lead to enzyme inhibition, given the generally increased stability of NO complexes with ferrous haem compared with those formed with ferric haem.

The recent suggestion that cytochrome *c* is released into the cytoplasm during apoptosis [43,44] has increased interest in the reactivity of cytochrome *c*. Given that NO can induce apoptosis [45], it is not impossible to conceive of conditions where NO and ferrocytochrome *c* produce NO^- in the cytoplasm, which could act as a distinct messenger/signal to NO by reacting with ferric, rather than ferrous, haem.

The formation of NO^- from ferrocytochrome *c* and NO may also explain the high-affinity inhibition of cytochrome *c* oxidase by NO. NO is a better inhibitor of cytochrome *c* oxidase in the steady state than one would expect from the binding of NO to isolated enzyme [46,47]. NO binds readily to reduced haem a_3 at the oxygen-reduction site of cytochrome oxidase, but the reported K_i of 60 nM at 30 μM oxygen [18] is over 5 times greater than that expected from the measured on- and off-rates for NO to reduced haem a_3 [47]. However, it has been shown that NO^- binds to oxidized haem a_3 in cytochrome oxidase [48], generating the same haem nitrosyl complex that is known to be the final inhibited state of the enzyme following NO addition [46,47]. NO^- may therefore be a more potent inhibitor of cytochrome oxidase than NO, because it binds to oxidized haem a_3 which is present in far higher concentrations than reduced haem a_3 under normal oxygen tensions. We are currently investigating this possibility.

NO is metabolized, and potentially detoxified, by mitochondria [21,49]. How significant are the reactions with cytochrome *c* to this metabolism? Our studies suggest that measurements that focus solely on NO decay rates may miss the formation of intermediate species and cycles. For example, NO metabolism to NO^- (e.g. by ferrocytochrome *c*) may be undetected if NO^- is subsequently reoxidized to NO by another mitochondrial enzyme or redox cofactor. This may partly explain why the NO decay rate in the presence of ferrocytochrome *c* is slower when cytochrome oxidase is also present, given that NO^- can bind to cytochrome oxidase, and the resulting ferrous haem a_3-NO complex can readily dissociate [47] to re-release more free NO into the solution.

Recent studies have suggested that cytochrome oxidase is the most significant metabolizer of NO in mitochondria. As illustrated in Figure 1, however, the presence of cytochrome oxidase does not increase the rate of NO removal from a solution containing a high concentration of reduced cytochrome *c*. Applying this to the mitochondrial situation is complicated, however, by the increased ratio of cytochrome *c*-to-cytochrome oxidase used in this study, compared with that in mitochondria. It is likely, however, that NO reactions with cytochrome *c* could explain some aspects of the mitochondrial NO metabolism, especially those which are insensitive to inhibitors of cytochrome oxidase, such as cyanide and azide. Indeed, the observed stronger inhibition [21] of NO metabolism by high (1 mM) cyanide concentrations when compared with high azide (10 mM) may be due to some formation of the cyanocytochrome *c* complex in the former case preventing redox cycling of the cytochrome *c*, and consequent NO breakdown. The relative importance of cytochrome *c* to mitochondrial NO metabolism could be determined by performing experiments using cytochrome-*c*-depleted mitochondria.

Given that the cytochrome *c* concentrations used here are within the physiological range in tissues (about 5–20 μM), the rate of the NO reaction with ferrocytochrome *c* is not high enough to explain the observed $t_{\frac{1}{2}}$ of NO in the perfused heart of 0.13 s [21], although the more rapid reaction of NO with ferricytochrome *c* might provide a sink for small concentrations of NO. However, the reaction of NO with ferricytochrome *c* is not rapid enough to act as a barrier to NO passage either in or out of the mitochondrion. Using a diffusion coefficient (*D*) for NO of 4.8×10^{-5} cm$^2 \cdot$s^{-1}, a ferricytochrome *c* concentration of 2 mM and a rate of NO binding of 1.3×10^3 M$^{-1} \cdot$s^{-1}, the mean diffusion distance for NO in the intermembrane space can be calculated [50] to be 80 μm.

In conclusion, we have demonstrated that an understanding of the interactions of NO with mitochondria cannot be restricted solely to the direct reactions of NO with cytochrome *c* oxidase, but must include those of its substrate as well.

This work was supported by a Wellcome Trust University Award to C. E. C. We thank Mike Wilson, Jaume Torres and Peter Nicholls (University of Essex) for helpful discussions.

REFERENCES

1 Knowles, R. G. and Moncada, S. (1994) Biochem. J. **298**, 249–258
2 Moncada, S., Palmer, R. M. J. and Higgs, E. A. (1991) Pharmacol. Rev. **43**, 109–142
3 Lewis, R. S. and Deen, W. M. (1994) Chem. Res. Toxicol. **7**, 568–574
4 Kelm, M. and Yoshida, K. (1996) in Methods in Nitric Oxide Research (Feelisch, M. and Stamler, J. S., eds.), pp. 47–58, John Wiley, Chichester
5 Kader, A., Frazzini, V., Solomon, M. D. and Tifiletti, R. (1993) Stroke **24**, 1709–1716
6 Iadecola, C., Xu, X. H., Zhang, F. Y., El-Fakahany, E. E. and Ross, M. E. (1995) J. Cereb. Blood Flow Metab. **15**, 52–59
7 Dawson, V. L. and Dawson, T. M. (1996) J. Chem. Neuroanat. **10**, 179–190
8 Matheis, G., Sherman, M. P., Buckberg, G. D., Haybron, D. M., Young, H. H. and Ignarro, L. J. (1992) Amer. J. Physiol **262**, H616–H620
9 Hogg, N., Darley-Usmar, V. M., Graham, A. and Moncada, S. (1993) Biochem. Soc. Trans. **21**, 358–362
10 Kooy, N. W., Royall, J. A., Ye, Y. Z., Kelly, D. R. and Beckman, J. S. (1995) Am. J. Resp. Crit. Care Med. **151**, 1250–1254
11 Pfeiffer, S., Gorren, A. C. F., Schmidt, K., Werner, E. R., Hansart, B., Bohle, D. S. and Mayer, B. (1997) J. Biol. Chem. **272**, 3465–3470
12 Hogg, N., Singh, R. J. and Kalyanaraman, B. (1996) FEBS Lett. **382**, 223–228
13 Wink, D. A. and Feelisch, M. (1996) in Methods in Nitric Oxide Research (Feelisch, M. and Stamler, J. S., eds.), pp. 403–412, John Wiley, Chichester

14 Tyler, D. D. (1975) Biochem. J. **147**, 493–504
15 Schweizer, M. and Richter, C. (1994) Biochem. Biophys. Res. Commun. **204**, 169–175
16 Cleeter, M. W. J., Cooper, J. M., Darley-Usmar, V. M., Moncada, S. and Schapira, A. H. V. (1994) FEBS Lett. **345**, 50–54
17 Takehara, Y., Kanno, T., Yoshioka, T., Inoue, M. and Utsumi, K. (1995) Arch. Biochem. Biophys. **323**, 27–32
18 Brown, G. C. and Cooper, C. E. (1994) FEBS Lett. **356**, 295–298
19 Cooper, C. E. and Brown, G. C. (1995) Biochem. Biophys. Res. Commun. **212**, 404–412
20 Brown, G. C. (1995) FEBS Lett. **369**, 136–139
21 Borutaité, V. and Brown, G. C. (1996) Biochem. J. **315**, 295–299
22 Zhao, X.-J., Sampath, V. and Caughey, W. S. (1995) Biochem. Biophys. Res. Commun. **212**, 1054–1060
23 Brudvig, G. W., Stevens, T. H. and Chan, S. I. (1980) Biochemistry **19**, 5275–5285
24 Ignarro, L. J., Fukuto, J. M., Griscavage, J. M. and Rogers, N. E. (1993) Proc. Natl. Acad. Sci. U.S.A. **90**, 8103–8107
25 Kuboyama, M., Yong, F. C. and King, T. E. (1972) J. Biol. Chem. **247**, 6375–6383
26 Ascenzi, P., Coletta, M., Santucci, R., Polizio, F. and Desidieri, A. (1994) J. Inorg. Biochem. **53**, 273–280
27 Butt, W. D. and Keilin, D. (1962) Proc. R. Soc. London, Ser. B. **156**, 429–458
28 Orii, Y. and Shimada, H. (1978) J. Biochem. (Tokyo) **84**, 1543–1522
29 Dupre, S., Brunori, M., Wilson, M. T. and Greenwood, C. (1974) Biochem. J. **141**, 299–304
30 Murphy, M. E. and Sies, H. (1991) Proc. Natl. Acad. Sci. U.S.A. **88**, 10860–10864
31 Bonner, F. T. and Pearsall, K. A. (1982) Inorg. Chem. **21**, 1973–1978
32 Doyle, M. P., Mahapatro, S. N., Broene, R. D. and Guy, J. K. (1988) J. Am. Chem. Soc. **110**, 593–599
33 Dutta, D. and Landolt, D. (1972) J. Electrochem. Soc. **119**, 1320–1325
34 Kon, H. (1969) Biochem. Biophys. Res. Commun. **35**, 423–427
35 Kooy, N. W., Royall, J. A., Ischiropoulos, H. and Beckman, J. S. (1994) Free Radical Biol. Med. **16**, 149–156
36 Ehrenberg, A. and Szczepkowski, T. W. (1978) Acta Chem. Scand. **14**, 1684–1692
37 Malinski, T., Bailey, F., Zhang, Z. G. and Chopp, M. (1993) J. Cereb. Blood Flow Metab. **13**, 355–358
38 Tominaga, T., Sato, S., Ohnishi, T. and Ohnishi, S. T. (1994) J. Cereb. Blood Flow Metab. **14**, 715–722
39 Brown, G. C., Bolanos, J. P., Heales, S. J. R. and Clark, J. B. (1995) Neurosci. Lett. **193**, 201–204
40 Lipton, S. A., Choi, Y. B., Pan, Z. H., Lei, S. Z., Chen, H. S. V., Sucher, N. J., Loscalzo, J., Singel, D. J. and Stamler, J. S. (1993) Nature (London) **364**, 626–632
41 Stamler, J. S., Singel, D. J. and Loscalzo, J. (1992) Science **258**, 1898–1902
42 Westenberger, U., Thanner, S., Ruf, H. H., Gersonde, K., Sutter, G. and Trentz, O. (1990) Free Radical Res. Commun. **11**, 167–178
43 Liu, X. S., Kim, C. N., Yang, J., Jemmerson, R. and Wang, X. D. (1996) Cell **86**, 147–157
44 Kroemer, G., Zanzami, N. and Susin, S. A. (1997) Immunol. Today **18**, 44–51
45 Shimaoka, M., Iida, T., Ohara, A., Taenaka, N., Mashimo, T., Honda, T. and Yoshiya, I. (1995) Biochem. Biophys. Res. Commun. **209**, 519–526
46 Torres, J., Darley-Usmar, V. and Wilson, M. T. (1995) Biochem. J. **312**, 169–173
47 Guiffre, A., Sarti, P., D'Itri, E., Buse, G., Soulimane, T. and Brunori, M. (1996) J. Biol. Chem. **271**, 33404–33408
48 Mahapatro, S. N. and Robinson, N. C. (1988) J. Cell Biol. **619**, 3510
49 Clarkson, R. B., Norby, S. W., Smirnov, A., Boyer, S., Vahidi, N., Nims, R. W. and Wink, D. A. (1995) Biochim. Biophys. Acta **1243**, 496–502
50 Beckman, J. S. (1996) in Nitric Oxide: Principles and Actions (Lancaster, J. J., ed.), p. 43, Academic Press, San Diego

Received 5 September 1997/5 February 1998; accepted 2 March 1998